

ENTROPY GENERATION OF AIDING MIXED THERMAL CONVECTION, BETWEEN TWO NON-PARALLEL VERTICAL PLATES WITH UNIFORM TEMPERATURE

by

Souad HADJADJ^{a*}, Salah SAOULI^b, and Aissa ABIDI SAAD^c

^aUniversity Kasdi Merbah, Ouargla, Algeria

^bCentral University Abdelhafid Boussouf, MILA, Algeria

^cUniversity Kasdi Merbah, Ouargla, Algeria

Original scientific paper

<https://doi.org/10.2298/TSCI160826176H>

In the aim to optimize the flow systems, a numerical simulation is carried out to investigate the entropy generation of the aiding mixed convection within two non-parallel vertical plates. The computational procedure is made by solving the laminar, steady and bi-dimensional continuity, momentum, and energy equations with the finite volume method. The plates are symmetrically heated with uniform temperature. The mixed convection flow in the heated vertical channel is studied for two aiding buoyancy conditions (upstream flow between hot plates and downstream flow between cold plates). The calculations are performed for several parameters such as Richardson number or buoyancy parameter (Gr/Re^2), Reynolds and Bejan numbers. The results showed that the velocity, temperature and entropy generation profiles within the channel are significantly affected by the later parameters.

Key words: *entropy generation, Richardson number, aiding mixed convection, nonparallel vertical plates*

Introduction

Several studies on the mixed convection flow of viscous and incompressible fluid between two non-parallel plates (Jeffery-Hamel flow) have been carried out. The main cause of interest in this type of flows, is not just for the fundamental nature of the problem, but also mainly from the fact that, it is encountered in many applications such as chimneys, solar panels, double-skin facades, Trombe wall, cooling, and heating installations as well.

Jeffery-Hamel flows has been widely studied, both experimentally and numerically, since the pioneering work of Millsaps and Pohlhausen [1] which was conducted in absence of body forces in 1953. The first numerical solution report about the same problem with the combined forced and free convection flow and heat transfer of a non-isothermal body exposed to a non-uniform free stream velocity, is performed by Sparrow *et al.* [2]. The authors subdivided the buoyancy parameter on three intervals to distinguish when the flow is considered as pure (either forced or free) or as mixed convection. In their study, two cases were considered, aiding and opposed convection inside convergent channel. Katkov [3] presented only one numerical solution for a very special case, the horizontal wall heated uniformly. Chen [4] tried to generalize the study of Jeffery Hamel flow induced by free convection in convergent divergent

* Corresponding author, e-mail: hadjadjsouad@gmail.com

channel. The channel is consisted of two non-parallel infinite porous plane walls where the used electrically conducting fluid is blown in or sucked out through these walls.

To better understand the mixed convection phenomenon in this flow system many experimental works have been carried out. Among others, Sparrow *et al.* [5] have performed an experimental study based on Nusselt number using water ($Pr = 5$) as working fluid. The results indicated that the Nusselt number for converged channel could be brought into very close agreement with those of parallel-walled channel by employing correlation variables based on the maximum wall spacing. Huang *et al.* [6] have visualized the flow structure inside a channel by heating a smoke wire. The effect of a large range of buoyancy parameter (from 0.3 to 907) and Reynolds number (from 100 to 4000) on the reversed flow structure for assisted and opposed convection is studied. The Nusselt number results are correlated in terms of relevant non-dimensional parameters for both pure and mixed convection. Bianco *et al.* [7] realized flow visualization of smoke inside non-parallel plates channel. The authors focused on the effect of minimal channel spacing, Rayleigh number ($2.85 \leq Ra \leq 1.22E + 05$) and the inclination angle ($0^\circ \leq \theta \leq 10^\circ$).

Other researchers treated and correlated this flow system numerically, using numerical computer codes such as Fluent and Phoenix, as Kaiser *et al.* [8], and Premachandran and Balaji [9].

Jeffery hamel flow in the presence of body forces needs more optimization in order to make the flow system more efficient with minimizing the energy losses. Using average Nusselt number correlations as in the study of Bianco *et al.* [10]. Or with another important way, which is the study of the entropy generation in the considered system where the fluid friction dissipation is added to the heat dissipation, to adjust all energetic system parameters and to know their dominance. Thus, it is crucial to gain a deeper knowledge and understanding of both dynamic and thermal behaviors of such systems. This research project is within the latter perspective, since, these flow systems (chimneys, double-skin façades, *etc.*) has got, and it is still getting, substantial attention from the researchers. This leads to the optimization and consequently developing a new efficient designs of such systems.

This new approach (entropy production) was studied in the first time by Shah [11], and Bejan [12-14]. Concerning the internal mixed and natural convection flows optimization was started recently, the vertical tube with uniform heat flux at the walls was studied by Ben-Man-sour *et al.* [15]. The vertical duct symmetrically heated with uniform temperature was assumed by Yang *et al.* [16]. The flow between vertical plates having imposed constant temperature was treated by Padet *et al.* [17]. The cavities was also studied by Salari *et al.* [18] and Sortigi and Hosseinizadeh [19]. The flow of Poiseuille-Benard was analyzed by Nouroollahi *et al.* [20].

The aim of the present work is to study numerically the entropy generation of the laminar aiding mixed convection flow and heat transfer in a symmetrically heated convergent channel. The two non-parallel channel walls were heated with uniform temperature. Numerical simulations have been performed with the commercial Fluent® CFD code based on finite volume method. This study is tempting to identify the causes of energy dissipation in such systems, since this flow is dissipative and irreversible.

The influence of several parameters on the heat transfer and fluid flow characteristics is considered *i. e.* buoyancy parameter (Gr/Re^2) ranging from 0.1-10 and Reynolds number from 10-200, using air as working fluid. The velocity and temperature distributions have been analyzed for two buoyancy aiding mixed convection conditions *i. e.* upstream flow between hot plates ($T_w - T_\infty > 0$), and downstream flow between cold plates ($T_w - T_\infty < 0$). Also, Bejan number is taken in consideration to confirm the dominance of one of two irreversible phenomena (the heat transfer or fluid friction) on the entropy generation.

Mathematical formulation

We considered laminar, assisted mixed convection, steady and incompressible flow of viscous and Newtonian fluid, between two non-parallel impermeable and isotherm plates (convergent channel).

The aiding buoyancy force has two cases [2, 21], fig. 1:

- Case 1: upstream flow between hot plates ($T_w - T_\infty > 0$).
- Case 2: downstream flow between cool plates ($T_w - T_\infty < 0$).

The variation of fluid thermophysical properties with temperature has been neglected with the exception of buoyancy term, for which the Boussinesq approximation has been adopted [2].

Governing equations, continuity, momentum, and energy in 2-D, are expressed as follows, respectively [2]:

$$\frac{\partial u}{\partial x} + \frac{\partial v}{\partial y} = 0 \quad (1)$$

$$\rho \left(u \frac{\partial u}{\partial x} + v \frac{\partial u}{\partial y} \right) = -\frac{\partial P}{\partial x} + \mu \left(\frac{\partial^2 u}{\partial x^2} + \frac{\partial^2 u}{\partial y^2} \right) \quad (2)$$

$$\rho \left(u \frac{\partial v}{\partial x} + v \frac{\partial v}{\partial y} \right) = -\frac{\partial P}{\partial y} + \mu \left(\frac{\partial^2 v}{\partial x^2} + \frac{\partial^2 v}{\partial y^2} \right) - \rho_\infty [1 - \beta(T - T_\infty)]g \quad (3)$$

$$u \frac{\partial T}{\partial x} + v \frac{\partial T}{\partial y} = \frac{k}{\rho C_p} \left(\frac{\partial^2 T}{\partial x^2} + \frac{\partial^2 T}{\partial y^2} \right) \quad (4)$$

The local entropy generation equation is written as [22]:

$$S_T = S_{\text{heat}} + S_{\text{fric}} \quad (5)$$

where S_{heat} and S_{fric} represent the entropy generation due to heat transfer and viscosity, respectively, which can be obtained from:

$$S_T = \frac{k}{T^2} \left[\left(\frac{\partial T}{\partial x} \right)^2 + \left(\frac{\partial T}{\partial y} \right)^2 \right] + \frac{\mu}{T} \left\{ 2 \left[\left(\frac{\partial u}{\partial x} \right)^2 + \left(\frac{\partial v}{\partial y} \right)^2 \right] + \left(\frac{\partial v}{\partial x} + \frac{\partial u}{\partial y} \right)^2 \right\} \quad (6)$$

The dimensional parameters used in this problem were: Reynolds number, Grashof number, Richardson number or buoyancy parameter, Nusselt number and Bejan number:

$$\text{Re} = \frac{\rho V_\infty D_h}{\mu}, \quad \text{Gr} = \frac{g \beta (T_w - T_\infty)}{\nu^2}, \quad \text{Ri} = \frac{\text{Gr}}{\text{Re}^2}, \quad \text{Nu} = \frac{h L}{k}, \quad \text{Be} = \frac{S_{\text{heat}}}{S_T}$$

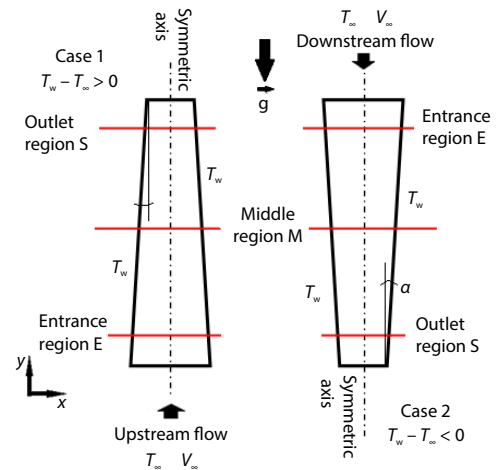


Figure 1. Schematics of the upstream and downstream flow

Physical description of the problem

This duct is based on experimental work of Huang *et al.* [6], with 45 cm in length and 5 cm in minimal spacing between plates at the outlet. The plates are tilted with 2° and heated uniformly in Case 1 or have the ambient temperature in the second case.

To simplify the treatment of this problem, we take only the half of the converging channel, as the plates have an equal temperature, whose the results are going to be symmetrical relative to the central axis.

The boundary conditions are established:

- at the entrance of the convergent: inlet velocity, v_∞ , and inlet fluid temperature, T_∞ ,
- at the exit of the convergent: outlet pressure (ambient pressure),
- at wall: wall temperature, T_w , and
- in the center: the symmetric axis.

Numerical solution

The coupled system of precedent governing eqs. (1)-(4) and (6) has been obtained by FLUENT code, based on a finite volume procedures according to SIMPLE algorithm. The equations are discretized on a staggered grid [23], using PRESTO scheme with a second order upwind scheme.

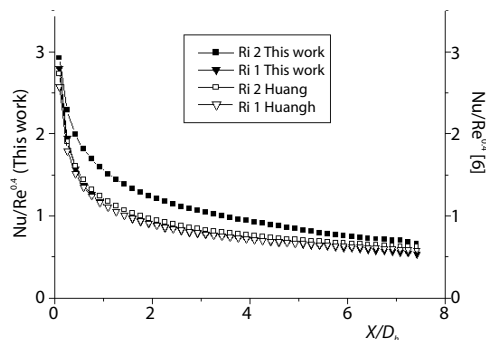


Figure 2. Comparison of present work with benchmark values

The grid distribution employed is 45 nodes (1 grid size) vertically and 16 nodes horizontally with 1.1 double size ratios to provide a finer mesh in the vicinity of the walls.

Code validation

The comparison of the local surface Nusselt number calculated by FLUENT code of this work and the one of the experimental studies of Huang *et al.* [6], calculated by their correlation (7), at $Re = 200$ and Richardson number takes two values 10 and 20. This comparison is shown in fig. 2, sufficient convergence was found with an average error of 2.22% between curves.

$$\frac{Nu}{Re^{0.4}} = 0.9232 \left(\frac{x}{D_h} \right)^{-0.3306} \left[1 + 0.086 \left(\frac{Gr}{Re^2} \right)^{0.42} \right] \quad (7)$$

Results and discussion

It is noted that the laminar aiding convection in the convergent channel depends on many parameters such as Richardson, Reynolds, Grashof, and Prandlt numbers, and the aspect ratio of the convergent channel. In this paper the effect of two parameters are considered on air-flow through a given size of duct, *i. e.*: Richardson number in the range of 0.1-10 to remain in mixed convection interval as used in [2, 21], and Reynolds number between 10 and 200 to not exceed the limits of the internal laminar flow [24]. Also, the used temperature difference is 50 K, the half of the opening angle is $\alpha = 2^\circ$ and the characteristic length is the maximum inter-plate spacing, D_h , at the inlet of the duct.

The velocity, the temperature and the entropy generation behaviors were discussed at three stages, at the entrance (E), the middle (M), and the outlet (S) regions in the convergent duct.

Velocity patterns

Generally in the heated upward flow or in the cooled downward flow, the velocity profiles have the same shapes in its flow direction, taking into account some slight magnitude differences [25], fig. 3.

For the first case where the vertical plates were heated uniformly, an acceleration of the fluid is noticed in the vicinity of the heated wall due to the aiding buoyancy force. In the second case, the fluid moves rapidly because it enters heated at 343 K in the channel, although it moves along the cold wall, it is the aiding convection effect. In the two cases the fluid in the core moves slowly.

For the small Richardson number or buoyancy parameter ($Ri = 0.1$), no reversal flow is found. When this parameter increases (to $Ri = 10$), the flow field becomes increasingly skewed as (Gr/Re^2) increases. The skewness is characterized by increased velocities in the flow direction near the wall, and by decreased velocities in the center of the duct [26], forming a V-shaped recirculation region, see fig. 4. The magnitudes and extents of the reversed flow increase with the buoyancy parameter, see fig. 3.

In general, the buoyancy parameter has the effect of causing the heated buoyant flow to move more rapidly, which leads to a deeper penetration of the reversed flow and wider re-circulating region. However, the increase of Reynolds number has the opposite effect of pushing the reversed flow downward. At this location the heated buoyant flow has become thinner and moved more rapidly that can make the recirculating region wider, as shown in fig. 4.

It is revealed that the increase of Gr/Re^2 can promote the flow reversal formation, whereas the increase of Reynolds number can promote its suppression.

In the middle region, compared with the entrance region, velocity profiles developed and the buoyancy effect becomes important, but near the exit of the convergent channel,

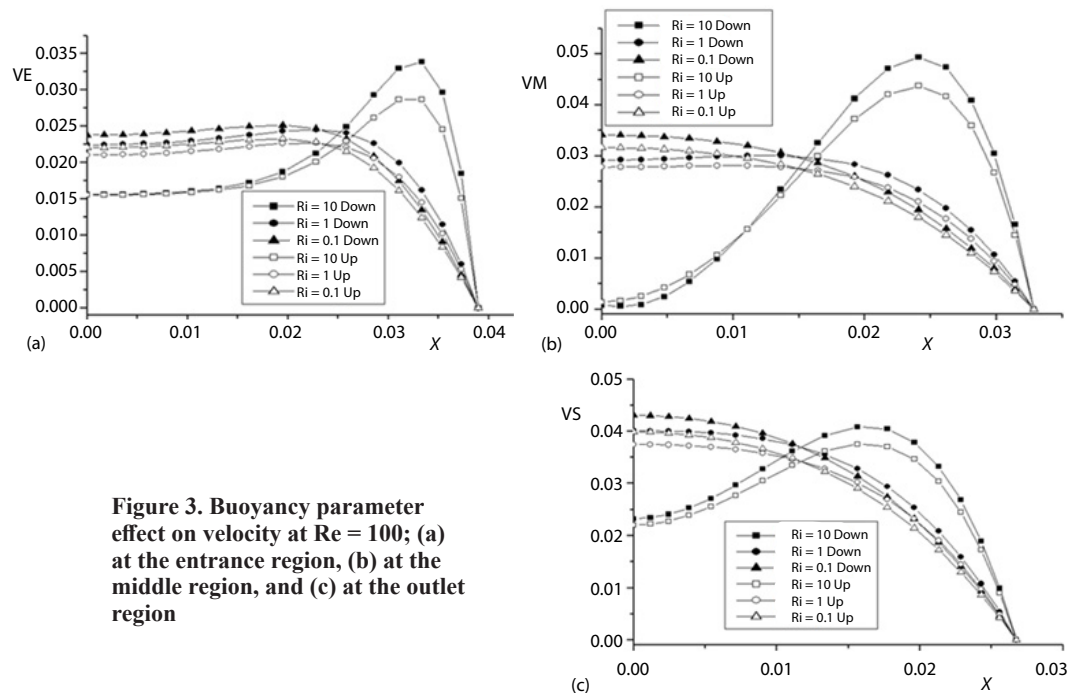


Figure 3. Buoyancy parameter effect on velocity at $Re = 100$; (a) at the entrance region, (b) at the middle region, and (c) at the outlet region

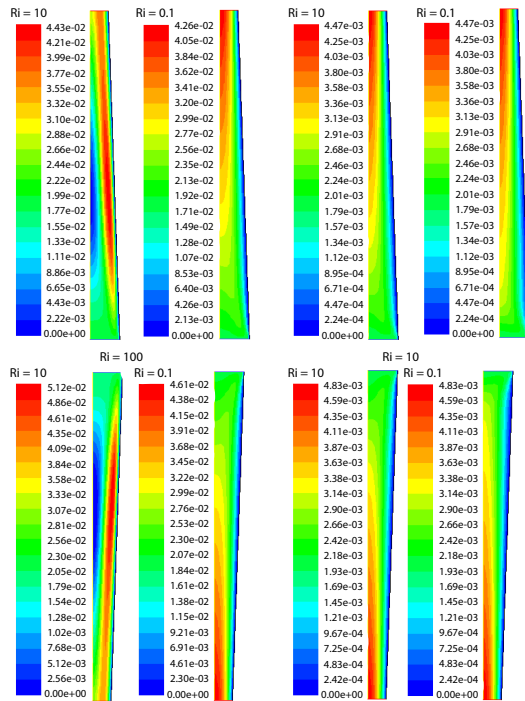
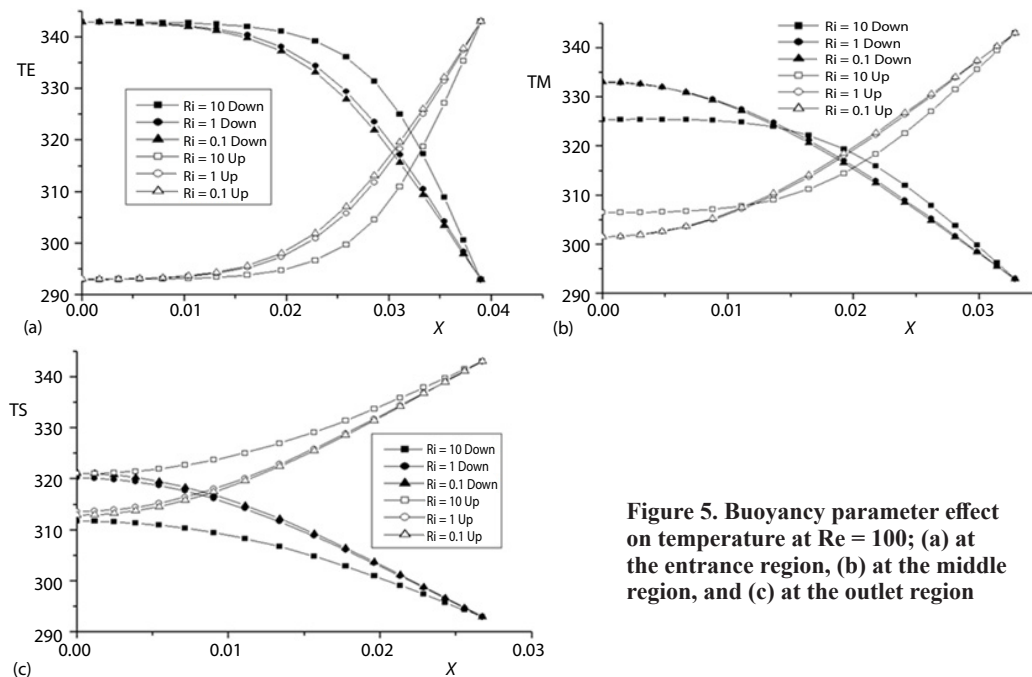


Figure 4. Stream-wise development of axial velocity for $Re = 10$ and 100 ; $Ri = 0.1$ and 10 , in two cases (upstream flow between hot plates and downstream flow between cold plates)



as shown in figs. 3(b) and 3(c), the flow accelerated and curves became less pronounced, this is due to the convergence of plates.

Temperature profiles

The results clearly indicate that buoyancy assisted flow can enhance the heat transfer process.

The boundary-layer of temperature distribution at the entrance region, fig. 5(a) displays the same simple shape that found in the thermal boundary-layer of the pure forced convection flows. In the middle of the duct, fig. 5(b), at large buoyancy parameter ($Ri = 10$), the fluid heats up or cools down. Also the more this parameter is increased the more the fluid gets or loses the heat.

In the entrance region, when Reynolds number is larger enough, the natural convection effect on the flow and heat transfer process is small, since the value of buoyancy parameter is relatively small and the physical process is dominated by forced convection. Then the fluid is heated

Figure 5. Buoyancy parameter effect on temperature at $Re = 100$; (a) at the entrance region, (b) at the middle region, and (c) at the outlet region

gradually along the duct. When Gr/Re^2 increase, the natural convection effect becomes significant and starts to dominate the physical process, see fig. 6. At lower Reynolds number, even the small Gr/Re^2 makes natural convection more dominant from the entrance of the convergent duct.

Entropy generation profiles

The maximum entropy generation due to heat transfer, S_{heat} , locates nearby the plates, where the heat transfer is the largest, then it decreases towards the center of the duct. At the entrance and middle regions, S_{heat} is influenced by the buoyancy parameter. It decreases considerably with the increase of Richardson number, especially in the center of the duct. Such behavior can be explained by the fact that the fluid temperature gradient in that region decreases or does not exist. As seen earlier, fig. 7(a), but in the vicinity of plates, under the buoyancy effect, the trends of S_{heat} reverses, it increases with the increase of the buoyancy parameter, to the surroundings of V-shaped re-circulation, cited in velocity patterns discussion. At the exit of the duct the entropy generation due to heat transfer decreases with an increase of Richardson number, without turning its trends nearby the walls where the heat transfer process is achieved, see fig. 5(a).

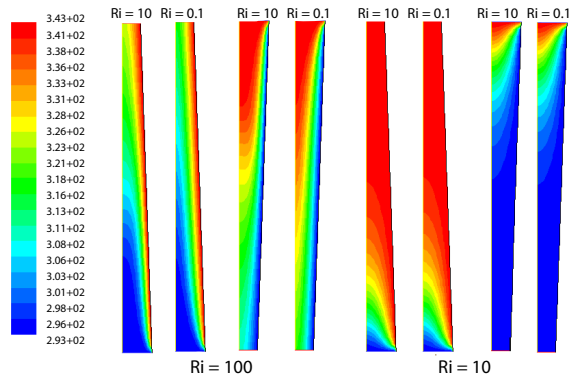


Figure 6. Temperature fields development for $Re = 10$ and 100 ; $Ri = 0.1$ and 10 , in two cases (upstream flow between hot plates and downstream flow between cold plates)

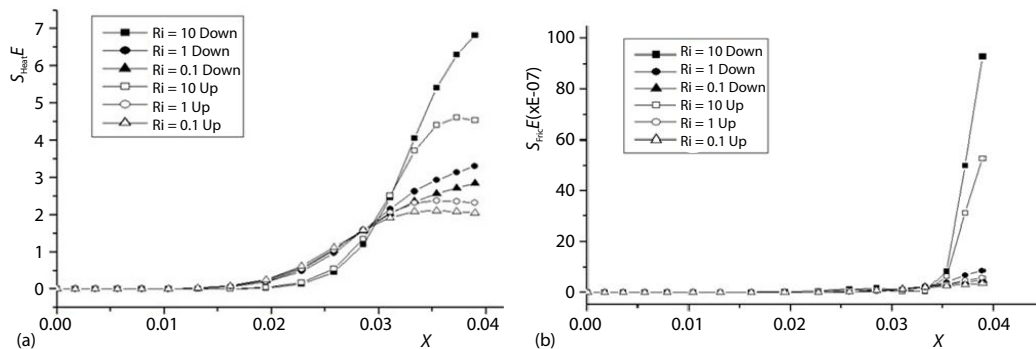


Figure 7. (a) Buoyancy parameter effect on S_{heat} at $Re = 100$ in the entrance region, (b) buoyancy parameter effect on S_{fric} at $Re = 100$ in the entrance region

In up-flow heating of fluid, the effect of free convection is to accelerate the velocity near the wall. To satisfy continuity, the velocity in the tube center is reduced [27]

When reversed flow occurs, the relatively lower velocity negative flow (in the tube center) hence carries a lower level of thermal energy. Since the net dimensionless mass-flow is fixed, an equal quantity of fluid is added to the fluid flowing in the positive (upward) direction and this flow adjacent to the hot wall thereby carrying a larger amount of energy [28].

Also S_{heat} is influenced by Reynolds number, as can be seen in fig. 8(a), the average S_{heat} (calculated by fluent) increases with an increase of Reynolds number. Moreover, in the fig. 7(a), the curves peaked and become bigger in the cooled downstream flow than that in the heated upstream flow.

Concerning the maximum values of the entropy generation due to fluid friction are always located at the channel walls, where the velocity gradient is the highest. Then it tends to zero toward the center of the convergent channel where the velocity gradient is small, fig. 7(b). The temperature difference in the channel is decreased by means of viscous dissipation effect due to the transformation of the fluid friction into heat. The S_{fric} increases with the increase of Richardson number along the convergent channel, and it increases from the inlet to the outlet under the effect of the convergence of plates, which accelerates the flow to the outlet, fig. 8(b). The effect of free convection is to increase the wall shear stress and that viscous dissipation is to reduce the same [27].

These maximum values are more important in the cooled upstream flow than those in the heated downstream flow. The effect of viscous dissipation is to augment heat transfer when the solid surface is cooled and to inhibit heat transfer when the solid surface is heated [27]. Also, the convergence of the channel makes the flow in the downstream faster. Reasonably for the largest Reynolds number, the S_{fric} takes its maximum values.

The global entropy generation, fig. 9, takes more reaction of the S_{fric} along the convergent duct with buoyancy parameter and Reynolds number influence.

Figure 10 shows that the heat transfer irreversibility dominates at small Reynolds numbers from the inlet to the outlet of the convergent channel, whatever the buoyancy parameter.

Bejan number

The Bejan number ranges from 0 to 1. Accordingly, $Be = 1$ is the limit at which the heat transfer irreversibility dominates, while $Be = 0$ is the opposite limit at which the irrevers-

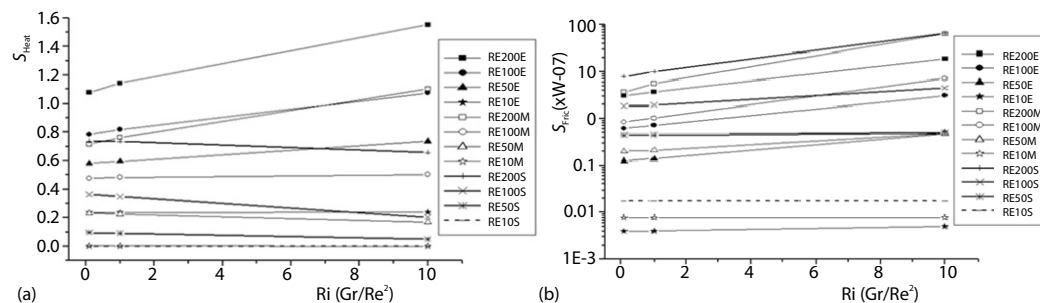


Figure 8. (a) Effect of Re and Ri on the average S_{heat} in all the duct, (b) effect of Re and Ri on the average S_{fric} in all the duct

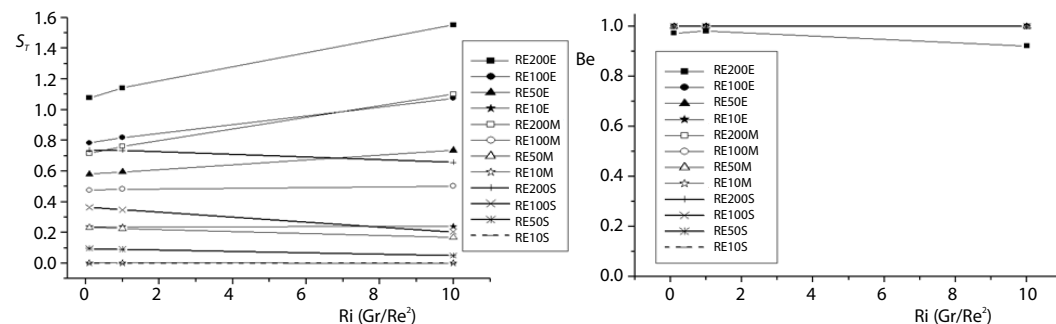


Figure 9. Effect of Re and Ri on the average S_T in all the duct

Figure 10 : Effect of Re and Ri on the average Be in all the duct

ibility is dominated by fluid friction effects and $Be = 1/2$ is the case at which the heat transfer and fluid friction entropy generation rates are equal [29].

Figure 10 shows that the heat transfer irreversibility dominates at small Reynolds numbers from the inlet to the outlet of the convergent channel, whatever the buoyancy parameter. When Reynolds number becomes large enough ($Re = 200$), the heat transfer irreversibility begins to dominate.

Conclusions

In this paper, the energy dissipation induced by the laminar aiding mixed convection flow within a convergent channel was studied numerically, using a finite volume method based code (FLUENT). The channel plates are non-parallel and symmetrically heated with uniform temperature. The present study focused more specifically on the buoyancy parameter and Reynolds number effects. Two cases are considered each one has a buoyancy condition *i. e.* heated upstream and cooled downstream flows.

The subsequent is a concise summary of the core results of this study.

- The converging of the plate decreases the entropy generation inside the channel. Also, at the channel inlet, the aiding buoyancy force promotes both the reversed flow occurrence and the heat transfer between the channel walls and the fluid. Also, the heat transfer irreversibility dominates much more in the vicinity of the channel walls especially for the lower Reynolds number.
- Often the local entropy generation takes more the behaviours of the heat transfer irreversibility, which implies the dominance of this latter. This finding is confirmed by Bejan number plots.

Nomenclature

Be	– Bejan number, ($= S_{\text{heat}}/S_f$)
C_p	– specific heat of the fluid, [$\text{J}\cdot\text{K}^{-1}$]
D_h	– characteristic length, [m]
Gr	– Grashof number [$= g\beta(T_w - T_\infty)D_h^3/\nu^2$], [–]
g	– acceleration due to gravity, [$\text{m}\cdot\text{s}^{-2}$]
h	– convective heat transfer coefficient, [$\text{W}\cdot\text{m}^{-2}\cdot\text{K}^{-1}$]
k	– thermal conductivity, [$\text{W}\cdot\text{m}^{-1}\cdot\text{K}^{-1}$]
L	– plate length, [m]
Nu	– Nusselt number ($= hL/k$), [–]
P	– pressure, [Nm ⁻²]
Pr	– Prandtl number ($= \mu C_p/k$), [–]
Re	– Reynolds number ($= \rho V_\infty D_h/\mu$), [–]
Ri	– Richardson number ($= Gr/Re^2$)
S_f	– entropy generation, [$\text{W}\cdot\text{m}^{-3}\cdot\text{K}^{-1}$]
S_{fric}	– energy dissipation due to fluid friction, [$\text{W}\cdot\text{m}^{-3}\cdot\text{K}^{-1}$]

S_{heat}	– energy dissipation due to heat transfer, [$\text{W}\cdot\text{m}^{-3}\cdot\text{K}^{-1}$]
T	– temperature, [K]
T_w	– plates temperature, [K]
T_∞	– inlet temperature, [K]
u, v	– velocity components along x, y , [$\text{m}\cdot\text{s}^{-1}$]
V_∞	– inlet velocity, [$\text{m}\cdot\text{s}^{-1}$]
x, y	– cartesian co-ordinates, [m]

Greek symbols

α	– half of the opening angle, [°]
β	– volumetric coefficient of expansion, [K^{-1}]
ρ	– density of the fluid, [$\text{kg}\cdot\text{m}^{-3}$]
μ	– fluid dynamic viscosity, [$\text{kg}\cdot\text{m}^{-1}\cdot\text{s}^{-1}$]
ν	– kinematic viscosity, [$\text{m}^2\cdot\text{s}^{-1}$]

References

- [1] Millasaps, K., Pohlhausen, K., Thermal Distributions in Jeffery-Hamel Flows between Nonparallel Plane Walls, *The Aeronautical Sciences*, 20 (1953), 3, pp. 187-196
- [2] Sparrow, E. M., *et al.*, Combined Forced and Free Convection in Boundary-Layer Flow, *The Physics of Fluids*, 2 (1959), 3, pp. 319-328
- [3] Katkov, V. L., Exact Solutions of Certain Convection Problems, *PMM*, 32 (1968), 3, pp. 482-487
- [4] Chen, T. H., Jeffery-Hamel Flow with Free Convection, Ph. D. thesis, University of Nebraska, Lincoln, Ore., USA, 1973

- [5] Sparrow, E. M., *et al.*, Experimental and Numerical Investigation of Natural Convection in Convergent Vertical Channel, *Inter. Journal of Heat and Mass Transfer*, 31 (1988), 5, pp. 907-915
- [6] Huang, T. M., *et al.*, Mixed Convection Flow and Heat Transfer in Heated Vertical Convergent Channel, *Heat and Mass Transfer*, 38 (1995), 13, pp. 2445-2456
- [7] Bianco, N., *et al.*, Experimental Investigation on Natural Convection in Convergent Channel with Uniformly Heated Plates, *Heat and Mass Transfer*, 50 (2007), 13-14, pp. 2772-2786
- [8] Kaiser, A. S., *et al.*, Correlation for Nusselt Number in Natural Convection in Vertical Convergent Channel at Uniform Wall Temperature by a Numerical Investigation, *Heat and Fluid Flow*, 25 (2004), 4, pp. 671-682
- [9] Premachandran, B., Balaji, C., A Correlation for Mixed Convection Heat Transfer from Converging, Parallel and Diverging Channels with Uniform Volumetric Heat Generating Plates, *Inter. Comunic. in Heat and Mass Transfer*, 33 (2006), 3, pp. 350-356
- [10] Bianco, N., *et al.*, Thermal Design and Optimization of Vertical Convergent Channels in Natural Convection, *Applied Thermal Engineering*, 26 (2006), 2-3, pp. 170-177
- [11] Shah, R. K., *et al.*, *Laminar Flow Forced Convection in Ducts*, Academic Press, New York, USA, 1978
- [12] Bejan, A., A Study of Entropy Generation in Fundamental Convective Heat Transfer, *Heat Transfer*, 101 (1979), 4, pp. 718-725
- [13] Bejan, A., Second-Law Analysis in Heat Transfer and Thermal Design, *Heat Transfer*, 15 (1982), Dec., pp. 1-58
- [14] Bejan, A., *Entropy Generation Minimization*, CRC, Boca Raton, Fla., USA, 1996
- [15] Ben-Mansour, R., *et al.*, Dissipation and Entropy Generation in Fully Developed Forced and Mixed Laminar Convection, *Inter. Jour. of Thermal Science*, 45 (2006), 10, pp. 998-1007
- [16] Yang, G., *et al.*, Flow Reversal and Entropy Generation Due to Buoyancy Assisted Mixed Convection in the Entrance Region of a Three Dimensional Vertical Rectangular Duct, *Inter. Jour. of Heat and Mass Transfer*, 67 (2013), Dec., pp. 741-751
- [17] Padet, C., *et al.*, Analysis of the Developed Mixed Thermal Convection by Use of 2nd Law, *Bulletin of the Transilvania University of Brasov*, 2 (2009), 51, pp. 227-234
- [18] Salari, M., *et al.*, Effects of Circular Corners and Aspect-Ratio on Entropy Generation Due to Natural Convection of Nanofluid Flows in Rectangular Cavities, *Thermal Science*, 19 (2015), 5, pp. 1621-1632
- [19] Sourtiji, E., Hosseiniadeh, S. F., Heat Transfer Augmentation of Magnetohydrodynamics Natural Convection in I-Shaped Cavities Utilizing Nanofluids, *Thermal Science*, 16 (2012), 2, pp. 489-501
- [20] Nourollahi, M., *et al.*, Numerical Study of Mixed Convection and Entropy Generation in the Poiseuille-Bernard Channel in Different Angles, *Thermal Science*, 14 (2010), 2, pp. 329-340
- [21] Cengel, Y. A., *Heat Transfer: A Practical Approach*, McGraw-Hill, New York, USA, 2003
- [22] Feidt, M., Thermodynamique et optimisation energetique des systemes et des procedés, (Thermodynamic and Energetic Optimisation of System and Methods – in French), 2nd ed., TECDOC, Paris, France, 1996
- [23] Patankar, S. V., *Numerical Heat Transfer and Fluid Flow*, Hemisphere Publishing Corporation, New York, USA, 1980
- [24] Oosthuizen, H. P., Naylor, D., *An Introduction to Convective Heat Transfer Analysis*, WCB/McGraw-Hill, New York, USA, 1999
- [25] Lauriat, G., *et al.*, Convection Naturelle – Cas Particuliers (Natural Convection – Particular Cases – in French), af4081, Techniques de l'ingénieur (Technics of Engineer), Paris, France, 2014
- [26] Gau, C., *et al.*, Reversed Flow Structure and Heat Transfer Measurements for Buoyancy-Assisted Convection in a Heated Vertical Duct, *ASME of Heat Transfer*, 114 (1992), 4, pp. 928-935
- [27] Iqbal, M., *et al.*, Viscous Dissipation Effects on Combined Free and Forced Convection through Vertical Circular Tubes, *ASME Journal of Applied Mechanics*, 37 (1970), 4, pp. 931-935
- [28] Aung, W., Worku, G., Theory of Fully Developed, Combined Convection Including Flow Reversal, *ASME Journal of Heat Transfer*, 108 (1986), 2, pp. 485-488
- [29] Shohel, M., *et al.*, Second Law Analysis of Heat Transfer and Fluid Flow Inside a Cylindrical Annular Space, *Exergy*, 2 (2002), 4, pp. 322-329